

Numerical modelling for monitoring the hysteretic behaviour of CFRP-retrofitted RC exterior beam-column joints

Seyed S. Mahini^{1a} and Hamid R. Ronagh^{*2}

¹*Department of Civil and Environmental Engineering, The University of New England, Armidale, NSW 2351, Australia (Formerly Assist. Prof., Yazd University, Iran)*

²*School of Civil Engineering, The University of Queensland, Brisbane, QLD 4072, Australia*

(Received November 17, 2009, Accepted November 23, 2010)

Abstract. This paper presents the results of a study on the capability of nonlinear quasi-static finite element modelling in simulating the hysteretic behaviour of CFRP and GFRP-retrofitted RC exterior beam-column joints under cyclic loads. Four specimens including two plain and two CFRP/GFRP-strengthened beam-column joints tested by Mahini and Ronagh (2004) and other researchers are modelled using ANSYS. Concrete in compression is defined by the modified Hognestad model and anisotropic multi-linear model is employed for modelling the stress-strain relations in reinforcing bars while anisotropic plasticity is considered for the FRP composite. Both concrete and FRP are modelled using solid elements whereas space link elements are used for steel bars considering a perfect bond between materials. A step by step load increment procedure to simulate the cyclic loading regime employed in the testing. An automatically reforming stiffness matrix strategy is used in order to simulate the actual seismic performance of the RC concrete after cracking, steel yielding and concrete crushing during the push and pull loading cycles. The results show that the hysteretic simulation for all specimens is satisfactory and therefore suggest that the numerical model can be used as an inexpensive tool to design of FRP-strengthened RC beam-column joints under cyclic loads.

Keywords: reinforced concrete; joints; strengthening; fibre reinforced plastics; finite element method; nonlinear analysis; cyclic loads.

1. Introduction

Hysteretic behaviour of RC structure under cyclic loads can be used to simulate the behaviour of structures under actual earthquakes loads. The hysteretic behaviour can generally be divided into two groups: The narrow low strength hysteretic curve with limited energy dissipation capacity and ductility, and the wide high strength hysteretic curve with more ductility and energy dissipation.

Many existing reinforced concrete (RC) frames building located in seismic zones are deficient in withstanding moderate to severe earthquakes. Insufficient lateral resistance along with poor detailing of members and joint reinforcement are the main reasons for inadequate seismic performance of

*Corresponding author, Senior Lecturer, E-mail: h.ronagh@uq.edu.au

^aLecturer, E-mail: smahini@une.edu.au

these structures (Paulay and Priestley 1992). Designing beam-column joints is considered to be a complex and challenging task for structural engineers and careful design of joints in RC frame structures is crucial to the safety of the structure. Hence, particular attention to the ductility of the reinforcement within the joint region is necessary. If the joint is not designed properly, the possibility of plastic hinge formation in the columns increases substantially (Paulay and Priestley 1992). This is dangerous for two reasons; firstly the collapse mechanism associated with hinges in the columns has a lower ultimate load and secondly the energy absorbance of plastic hinges within the columns is normally less due to reinforcement arrangement and the axial load. Engineers can avoid this when designing Ductile Moment Resisting Frames (DMRFs) by employing the *weak-beam strong-column* principle (Mahini and Ronagh 2007). In recent years, several researches used externally bonded FRP composite in order to increase the shear, flexural and anchorage capacity of (RC) frame joints. For example, Ghobarah and Said (2001) tested a beam-column concrete exterior joint before and after GFRP retrofitting under cyclic loads. Ghobarah and Said (2001) concluded that GFRP retrofitting of the connection core causes an increase of the shear strength of the joint. In addition, Smith and Shrestha (2006) carried out a systematic review of experimental research on the FRP-strengthening of RC connections and evaluated the effectiveness of these strengthening schemes. They reported that four different types of FRP-strengthening including Shear Strengthening, Anchorage Strengthening, Shear and Anchorage Strengthening and Plastic Hinge Relocation have been introduced into connections. To the best of the authors' knowledge, no tests have been performed on using externally bonded FRP to relocate a plastic hinge further along the beam away from the column face. In this regard, Mahini *et al.* (2004) tested an exterior beam-column joint before and after reinforcement with CFRP web-bonded under cyclic loads. Mahini *et al.* (2004) concluded that the plain and FRP retrofitted connection have similar strength and ductility, but the reinforced connection has better energy dissipation due to the shifting of the plastic hinge away from the column face. Mahini and Ronagh (2006, 2007, 2009) also showed, that the web-bonded CFRP system (when carefully designed) could restore the strength and ductility of damaged joints and improve the brittle failure of beam column joints into a ductile manner by relocating the potential plastic hinge away from the column face towards the beam. Similar studies, but with other methods (such as the use of headed reinforcing bars) have been conducted on relocating plastic hinges away from the column faces (Chutarat and Aboutaha 2003).

Numerical modelling is also used to investigate into the hysteretic behaviour of RC beam-column joints. Recently, Parvin and Wu (2008) conducted a numerical analysis to investigate the effect of ply angle on the improvement of shear capacity and ductility of beam-column joint strengthened with CFRP wraps under combined axial and cyclic loads. In this study, the finite element analysis study entailed profiling the behaviour of three beam-column joint that were strengthened through the CFRP wrapping with various ply angle configuration. Parvin and Wu (2008) indicated that four layers of wrapping placed successively at $\pm 45^\circ$ ply angles with respect to the horizontal axis is the most suitable upgrade scheme for improving shear capacity and ductility of beam-column joints under combined axial and cyclic loads.

A comprehensive research study conducted at the University of Queensland on the ability of CFRP web-bonded systems in strengthening an exterior beam-column joint subjected to monotonic/cyclic loads (Mahini 2005). As part of this research, Mahini and Ronagh (2009) analysed one 1/2.2 scaled plain and four CFRP repaired/retrofitted joints subjected to monotonic loads using the nonlinear finite-element program ANSYS in order to calibrate the experiments. The ANSYS model was employed in order to account for tension stiffening in concrete after cracking and a modified

reinforcing steel bars, with two bars in the top and two bars in the bottom of the beam. All columns were reinforced with four N12 reinforcing bars, with one bar positioned in each corner of the column. The beam stirrups and column ties were 6.5 mm bars at 150 mm centres. Ties were also placed in the connection region in accordance with the earthquake loading requirements of AS3600 (2001). Additional stirrups and ties were placed near the ends of the beam and columns in all specimens to ensure local failure would not occur at the load and support points respectively. These specimens exhibit flexural failure modes. The proposed retrofitting system consists of three plies of web-bonded CFRP sheet. All layers were unidirectional sheets and were applied in a length of 200 mm from the column face on the beam-end with fibre directions parallel to the longitudinal beam axis as shown in Fig. 1.

T1 and T1R specimens represented full scale models. The height of the column and the length of the beam represent the distance to the contra flexure points in the frame. The column is 3000 mm high with cross-sectional dimensions of 250×400 mm. The beam's length is 1750 mm from the face of column to the free end with a cross-section of 250×400 mm. The longitudinal reinforcement used in the column is 6 M20 bars (equivalent to 19.5 mm diameter bar) in addition to 2 M15 bars (equivalent to 16.0 mm diameter bar) without splicing. The transverse reinforcement in the column is M10 rectangular ties with single M10 supplementary central leg. The ties start 80 mm above and below the beam and are spaced at 200 mm as shown in Fig. 2. Following the practice, before the seismic design codes were available, no transverse reinforcement was installed in the beam column joint. The top and bottom longitudinal reinforcement of the beam are 4 M20 bars each. The transverse reinforcement of the beam is M10 rectangular ties starting 75 mm from the face of column. The ties are spaced at 150 mm for 600 mm and then spaced at 200 mm for 1000 mm and ending at 75 mm from the free end of the beam. The beam-column joint is expected to fail in shear mode before a plastic hinge is formed in the beam due to the lack of transverse reinforcement in the joint. The beam-column joint specimen designated as T1 was tested as control specimen. The joint core was repaired and rehabilitated using one layer GFRP laminate in the form of "U" and then the test was conducted as shown in Fig. 2. The repaired and rehabilitated specimen is designated T1R.

2.2 Material properties

The concrete compressive strength; elastic modulus and splitting strength of CSC1 and RSC1 (see Table 1) were determined on the day of testing each connection. Yield strength of the N12 reinforcing steel bars and R6.5 mm stirrups and ties were also tested as being 500 MPa and 380 MPa respectively. Carbon fibers used had a thickness of 0.165 mm with a maximum elongation of 1.55% and a tensile strength of 3900 MPa according to the manufacturer's specifications.

The concrete compressive strength of T1 and T1R was on the day of the test of $f'_c = 30.8$ MPa. The reinforcing steel had a yield stress of $f'_y = 454$ MPa and 425 MPa for M10 and M20 bars, respectively. The Glass fibre (GFRP) properties listed in Table 2.

Table 1 Mechanical properties of concrete (Mahini *et al.* 2004)

Specimen	Compressive strength (MPa)	Modules of elasticity (GPa)	Tensile strength (MPa)
CSC1	40.73	30.17	3.29
RSC1	36.44	29.7	3.62

Table 2 Properties of GFRP (Ghobarah *et al.* 2001)

GFRP	Ultimate tensile strength (MPa)	Ultimate elongation (%)	Elastic modulus (MPa)	Thickness (mm)
Bi-directional (in the 45 direction)	552	1.7-4.0	27579	1.1

3. Finite element modelling

Three-dimensional nonlinear finite element models for the beam-column joints are developed using ANSYS (2005). To model the characteristics of concrete, Solid 65 element is used. This element is capable of simulating the cracking and crushing of concrete. The William-Varnk criterion was used for the fracture modelling of concrete. This model is able to account for the cracking of concrete in tension and crushing of concrete in compression. Some important parameters to perform the failure envelope in the model are the compressive strength of concrete, the modulus of the rupture, and the shear transfer coefficients for open and closed cracks. Also for modelling compressive strength of concrete, the Hognestad model was used. In addition, to model the longitudinal reinforcement and the FRP composites, Link 8 and Solid 45 elements are used, respectively. In order to model the FRP composites, an anisotropic material called ANISO is employed. To model the FRP material in both compression and tension and in any direction of X , Y and Z a bi-linear stress-strain curve was used. A multi-linear isotropic stress-strain curve was also considered for the stress-strain steel bars.

As no de-bonding was observed during the previous tests performed by the authors (Mahini *et al.* 2004), perfect bond between materials and concrete is considered for CSC1 and RSC1 so that adjacent elements have common nodes. The same approach also employed for T1 and T1R. In Fig. 3, two typical finite element models are shown for these specimens. Cyclic loads are applied

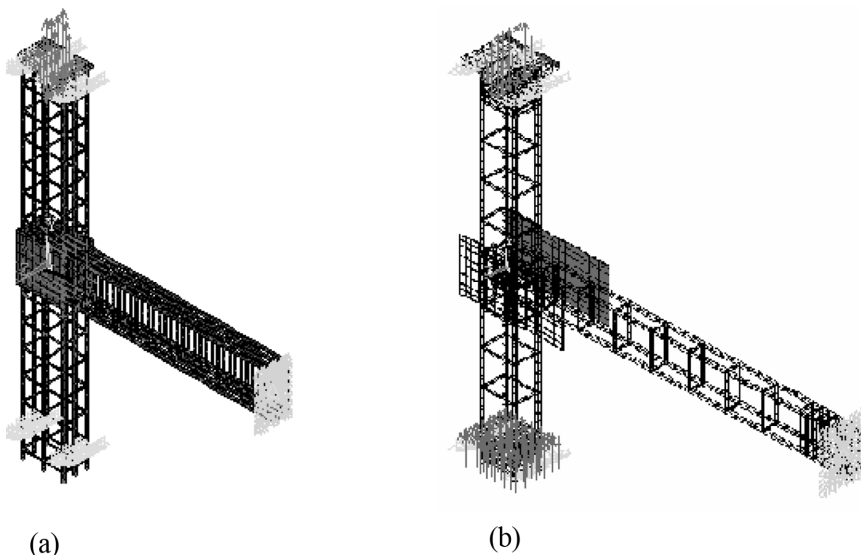


Fig. 3 Analytical specimen details (a) T1 and T1R (b) CSC1 and RSC1

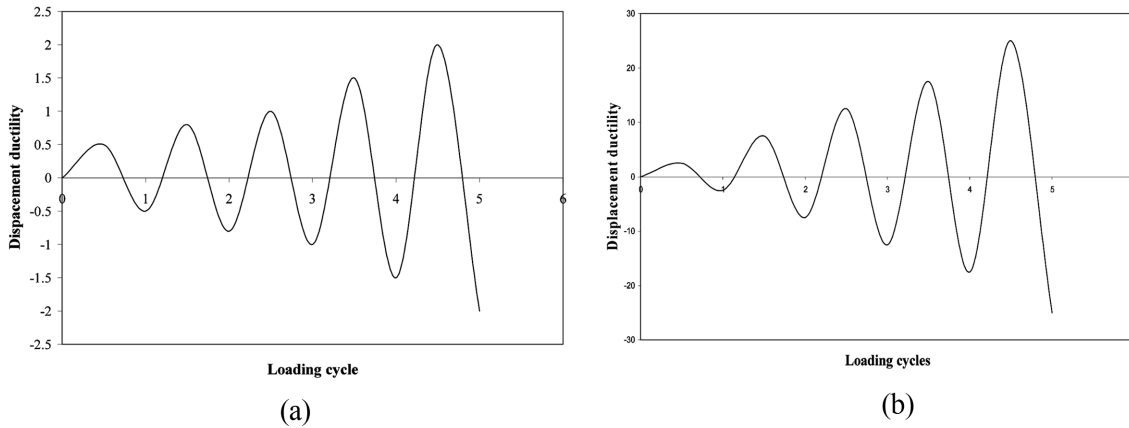


Fig. 4 Analytical loading regime (a) T1 and T1R (b) CSC1 and RSC1

with a step by step strategy in a displacement control regime similar to the tests as shown in Fig. 4. Each cycle is modelled in a load step and each load step is divided into a number of sub steps. At the initial step of the analysis, because the section is un-cracked and the solution is linear, a lower number of sub-steps are considered. However, at the cracking load and the final cycles, more load steps and sub-steps are utilized. An automatically reforming stiffness matrix is employed in order simulate cracking and crushing of the concrete and steel yielding during cyclic loading.

4. Comparison between experimental results and finite element models

4.1 Specimen CSC1

In the experimental study reported by Mahini *et al.* (2004), the plain specimen was loaded in two phases. The first phase included cycles that cause cracking and the second phases include cycles that cause first yielding of the longitudinal reinforcement followed by failure of joint. In the analytical modelling, this specimen is loaded similar to the experimental study. As is shown in Fig. 5, the plastic hinge was formed at the face of the column similar to the experimental observation. In Fig. 6, hysteretic curves of the specimen obtained from experimental and analytical studies are shown. As is seen, the experimental and numerical hysteretic curves are reasonably similar. The difference between these two could even become less distinguishable if a finer mesh is used in the numerical simulation.

Examining the hysteretic curves shows that in the analytical solution, the yield stress is reached at a displacement of 5 mm, where the maximum displacement and load are about 30.19 mm and 19.47 kN, respectively. In the experimental result, the displacement at yield and maximum displacement are equal to 5 mm and 26.6 mm, respectively with maximum load of 19.51 kN, as shown in Fig. 6. Also the envelopes of the beam tip load-displacement curves of experimental and numerical results is compared in Fig. 7.

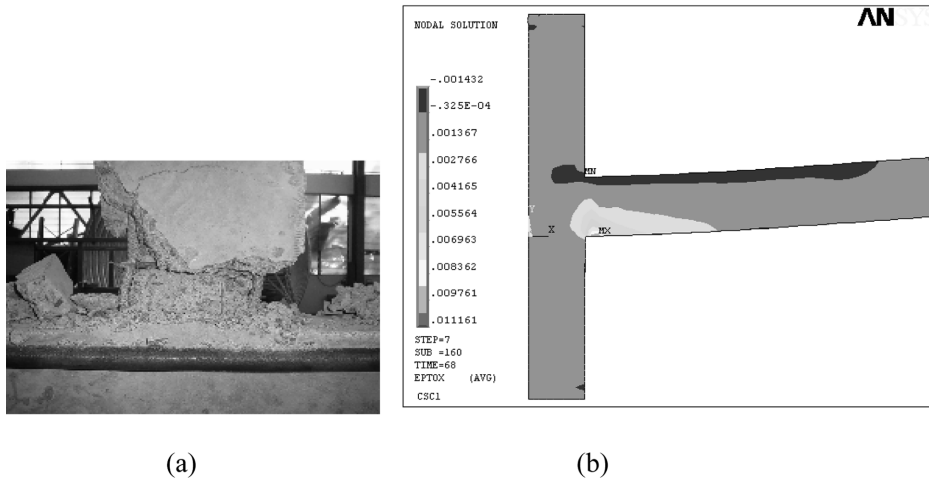


Fig. 5 (a) Observed and (b) obtained from numerical modelling failure mechanism of specimen CSC1 (Mahini *et al.* 2004)

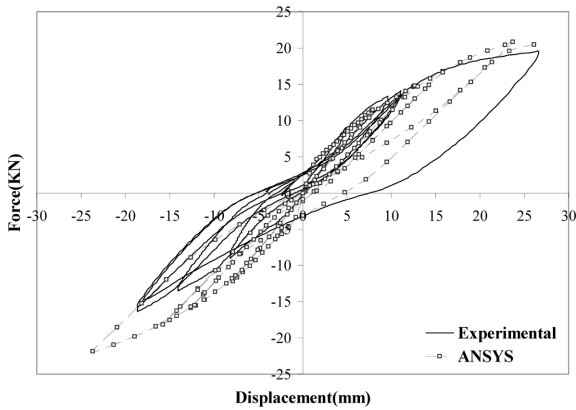


Fig. 6 Comparison between obtained hysteretic curves for plain specimen CSC1

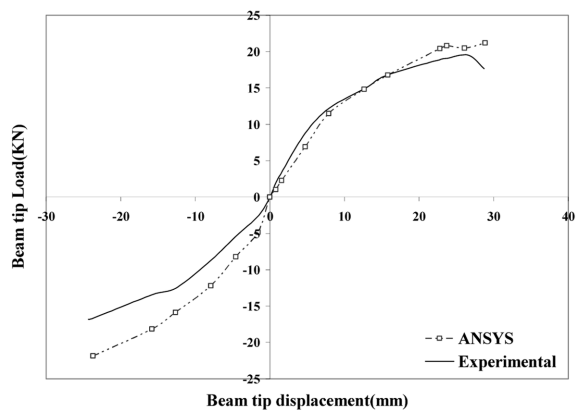


Fig. 7 Envelop of load versus displacement of CSC1 obtained from numerical analysis and experiment

4.2 Retrofitted specimen RSC1

Specimen RSC1 is subjected to the same loading regime as specimen CSC1. Fig. 8(a) shows the final failure of the specimen in which the plastic hinge formed beyond the cut-off point of the CFRP. In fact, CFRP reinforcement causes the plastic hinge moving from the face of column toward the beam. This can also be seen from numerical modelling (Fig. 8(b)) Comparison between both hysteretic curves obtained from the analytical and experimental show that the energy absorption is maintained as the maximum load is held to the end. The curves show that the first yield load of the analytical curve is equal to the experiment one (16 kN) and so is the maximum load (22 kN) as show in Fig. 9. Also the envelopes of the beam tip load-displacement curves of experimental and numerical specimen are shown, in Fig. 10.

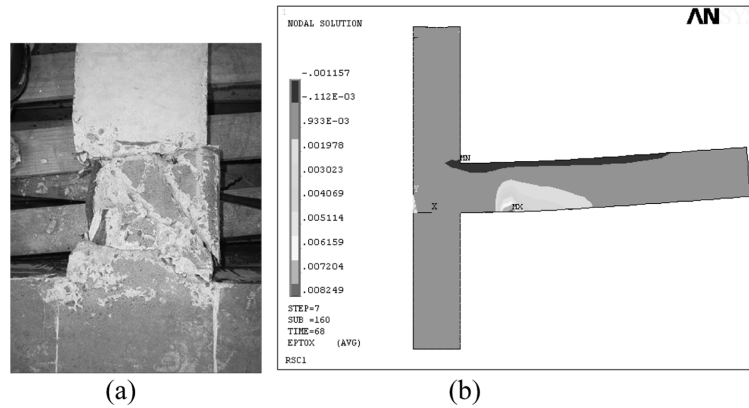


Fig. 8 (a) Observed and (b) obtained from numerical modelling failure mechanism of specimen RSC1 (Mahini *et al.* 2004)

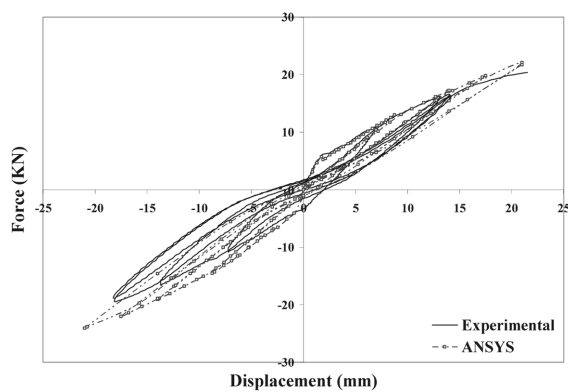


Fig. 9 Comparison between obtained hysteretic curve and numerical modelling of RSC1

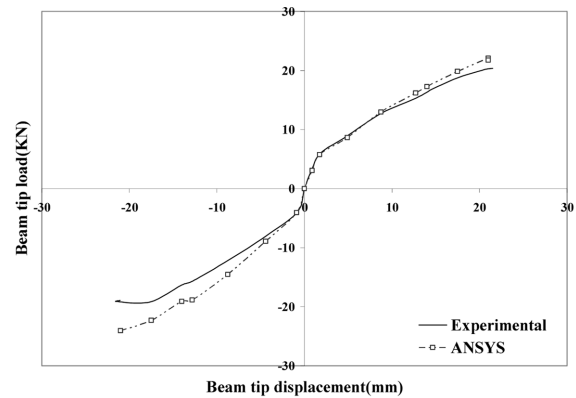


Fig. 10 Envelop of load versus displacement of RSC1 obtained from numerical analysis and experiment

4.3 Specimen T1

In the experimental study reported by Ghobarah *et al.* (2001), the specimen T1 was tested under reversed cyclic load applied at the beam tip. The selected load is intended to simulate high levels of inelastic deformation that may be experienced by the frame during a severe earthquake. The selected load history consists of two phases. The first phase is load-controlled loading phase and the second phase is displacement-controlled. In specimen T1, the first crack was recorded at the column face. Before first yield of longitudinal beam steel, diagonal shear crack was noted in the joint area in each loading direction forming an X-pattern as show in Fig. 11(a). In the analytical modelling, for which the loading was similar to the test specimen, the first crack was observed at the column face. Also at failure, shear cracks were diagonal in the joint core (Fig. 11(a)). Based on the analytical modelling, first yield stress of longitudinal beam steel happened in displacement 16.155 mm and loading of 111.2 kN. Also as Fig. 11(b) shows, failure strain in concrete is strain about 0.002.

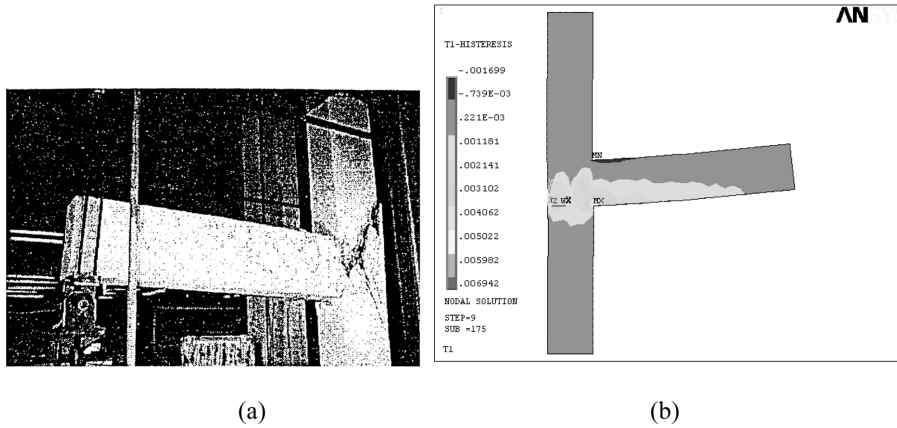


Fig. 11 (a) Observed and (b) obtained from numerical modelling failure mechanism of specimen T1 (Ghobarah *et al.* 2001)

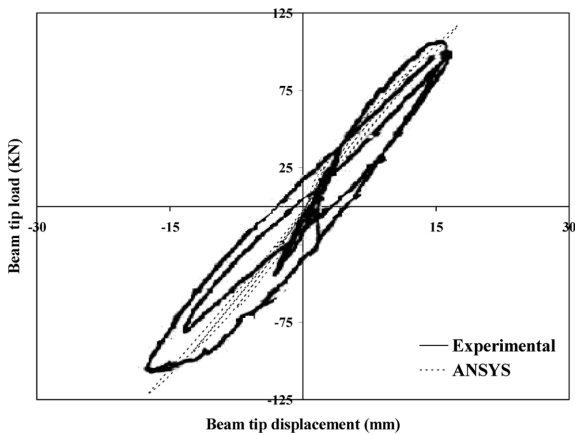


Fig. 12 Comparison between obtained hysteretic curves for plain specimen T1

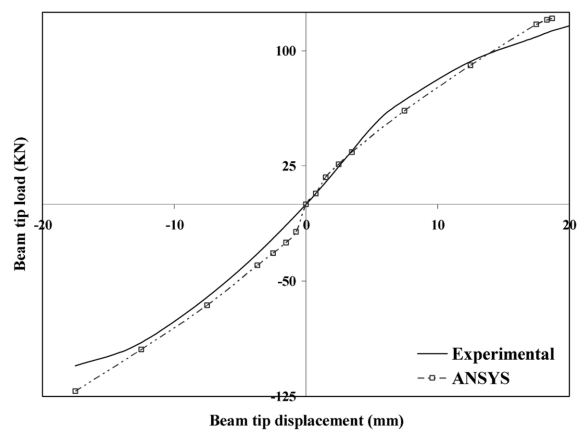


Fig. 13 Envelope of load versus displacement of T1 obtained for numerical and experimental

In Fig. 12, hysteretic curves of the specimen obtained from experimental and analytical studies is shown. In the experimental hysteretic curve pushing up load and down are 116.08 kN and 101.86 kN respectively, but in analytical hysteretic curve, these values are 116.97 kN and 121.94 kN. In addition, the envelope of the beam tip load-displacement curves of the experiment and the numerical analysis is shown in Fig. 13.

4.4 Specimen T1R

For numerical analysis of specimen T1R, the same loading regime as specimen T1 is used. As shown in Fig. 14, a similar failure mechanism is observed from experiment and numerical modelling. As is seen, a flexural plastic hinge in the beam of length that is approximately equal to the depth of the beam developed starting from the face of the column. As is also seen, using

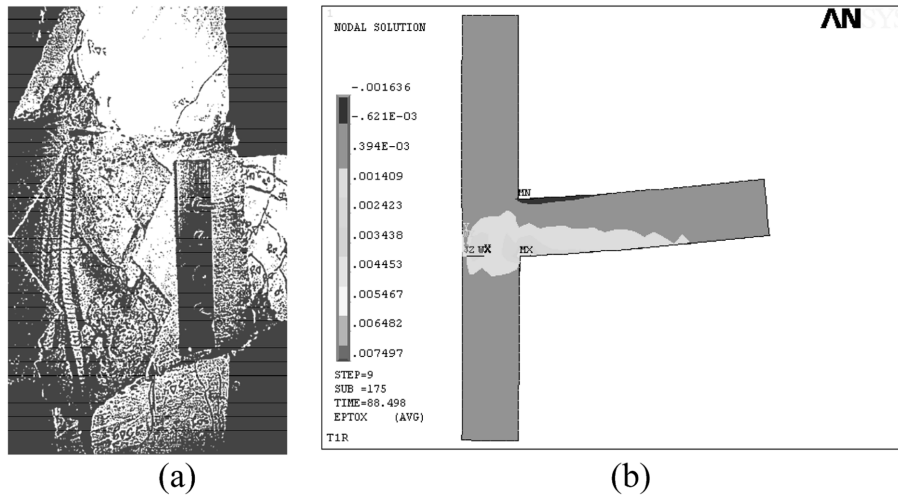


Fig. 14 (a) Observed and (b) obtained from numerical modelling failure mechanism of specimen T1R (Ghobarah *et al.* 2001)

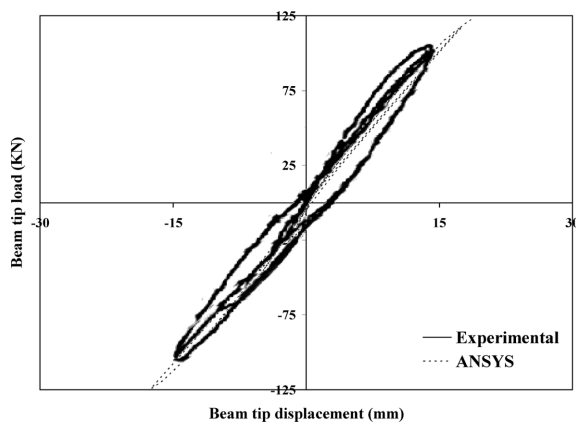


Fig. 15 Comparison between obtained hysteresis curve obtained from experiment and numerical modelling for T1R

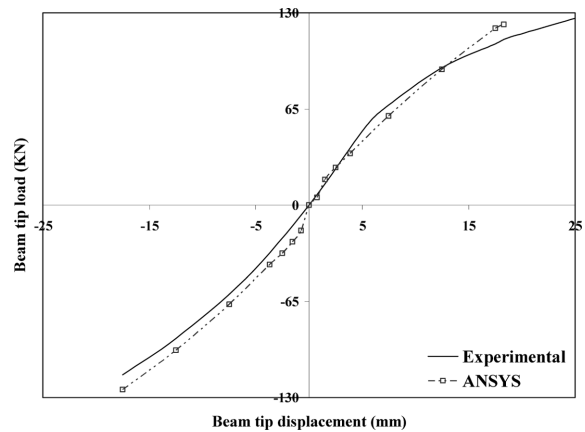


Fig. 16 Envelop of load versus displacement of T1R obtained from experiment and numerical analysis

GFRP plate in the joint has caused a recovery in the behaviour of the connection so that strain alteration in joint core is less than 0.002. In the analytical modelling, first yield stress of longitudinal beam steel has occurred at the displacement 15.741 mm and loading of 110 kN. As shown in Fig. 15, comparison between both hysteresis curves obtained from the analytical and experimental show that the up load and down load in experimental test are 126.23 kN and 114.61 kN respectively, but in the analytical hysteresis curve these are 128 kN and 124 kN. Also the envelopes of the beam tip load-displacement curves obtained from experimental and numerical results are shown in Fig. 16.

5. Conclusions

Based on the comparative modelling presented in this study, it is concluded that both hysteretic curves of the plain and retrofitted specimens are close to their experimental counterparts. This gives confidence to the design engineers and researchers in using finite element modelling for evaluating the cyclic performance of RC joints. Most effective retrofitting schemes can be easily found using the low cost finite element models similar to that presented in this study. The conclusion herein is only valid to the peak load, as concrete's strain softening cannot be modelled by ANSYS.

References

- ANSYS (2005), *ANSYS Manual Set*, ANSYS, Inc., Canonsburg, PA, USA.
- AS3600 (2001), *Concrete Structures*, Standards Australia, Homebush Bay, Australia.
- Chutarat, N. and Aboutaha, R.S. (2003), "Cyclic response of exterior reinforced concrete beam-column joints reinforced with headed bars-experimental investigation", *ACI Struct. J.*, **100**(2), 259-264.
- Ghobarah, A. and Said, A. (2001), "Seismic rehabilitation of beam-column joints using FRP laminates", *J. Earthq. Eng.*, **5**(1), 113-129.
- Mahini, S.S. (2005), "Rehabilitation of exterior RC beam-column joints using CFRP sheets", PhD thesis submitted to the Division of Civil Engineering of the University of Queensland, Australia.
- Mahini, S.S. and Ronagh, H.R. (2006), "Estimation of the ductility of web-bonded FRP beams for assessment of strengthened RC exterior joints", *Proceeding of the Third International Conference on FRP Composites in Civil Engineering (CICE 2006)*, Miami, December.
- Mahini, S.S. and Ronagh, H.R. (2007), "A new method for improving ductility in existing RC ordinary moment resisting frames using FRPs", *Asian J. Civil Eng., Build. Hous.*, **8**(6), 581-592.
- Mahini, S.S. and Ronagh, H.R. (2007), "Seismic upgrading of existing RC ordinary moment resisting frames using FRPs", *Proceeding of the First Asia-Pacific Conference on FRP in Structures (APFIS 2007)*, (Ed. Smith, S.T.), Hong Kong, December.
- Mahini, S.S. and Ronagh, H.R. (2009), "Numerical modelling of FRP strengthened RC beam-column joints", *Struct. Eng. Mech.*, **32**(5), 649-665.
- Mahini, S.S. and Ronagh, H.R. (2009), "Strength and ductility of FRP web-bonded RC beams for the assessment of retrofitted beam-column joints", *Compos. Struct.*, **92**(6), 1325-1332.
- Mahini, S.S., Dalalbashi Isfahani, A. and Ronagh, H.R. (2008), "Numerical modelling of CFRP-retrofitted RC exterior beam-column joints under cyclic loads", *Proceedings of Fourth International Conference on FRP Composites in Civil Engineering (CICE08)*, Zurich, July.
- Mahini, S.S., Ronagh, H.R. and Smith, S.T. (2004), "CFRP-retrofitted RC exterior beam-column connections under cyclic load", *Proceeding of the Second International Conference on FRP Composites in Civil Engineering*, Adelaide, December.
- Parvin, A. and Wu, S. (2008), "Ply angle effect on fibre composite wrapped reinforced concrete beam-column connections under combined axial cyclic loads", *Compos. Struct.*, **82**(4), 532-538.
- Paulay, T. and Priestley, M.J.N. (1992), *Seismic Design of Reinforced Concrete and Masonry Buildings*, John Wiley and Sons Inc.
- Smith, S.T. and Shrestha, R. (2006), "A review of FRP strengthened RC beam column connections", *Proceeding of the Third International Conference on FRP Composites in Civil Engineering (CICE 2006)*, Miami, December.